

# **On the development of unmodified mud grouts for repairing earth constructions: rheology, strength and adhesion**

R.A. Silva<sup>1</sup>, L. Schueremans<sup>2</sup>, D.V. Oliveira<sup>3</sup>, K. Dekoning<sup>4</sup>, T. Gyssels<sup>5</sup>

<sup>1,3</sup> *ISISE, University of Minho, Guimarães, Portugal*

<sup>2,4-5</sup> *Catholic University of Leuven, Heverlee, Belgium*

**Abstract:** The conservation and rehabilitation of several sites of cultural heritage and of the large housing stock built from earth requires the development of techniques and materials compatible with this kind of construction. Grout injection is one repair solution which has been put forward over the last few years, whereas there is preference for employing grouts that incorporate earth in their composition. However, knowledge of such grouts is still very limited and requires further research. The experimental program discussed in this paper contributes to the comprehension of the influence of the composition of an unmodified mud grout, namely regarding its fresh-state rheology, hardened-state strength and adhesion. In general, the results obtained showed that the rheological behaviour of a mud grout greatly depends on the colloid behaviour of the clay fraction, and that the addition of a deflocculant and modification of the clay content (with a silt size material) is required to obtain grouts with adequate solid fractions.

**Keywords:** Earth construction, mud grout, rheology, strength, adhesion

---

<sup>1</sup>PhD student, ISISE, University of Minho, Department of Civil Engineering, Azurém, P-4800-058 Guimarães, Portugal. Phone: +351 253 510 200, fax: +351 253 510 217, email: ruisilva@civil.uminho.pt

<sup>2</sup>PhD, Professor, Catholic University of Leuven, Department of Civil Engineering, P-3001, Heverlee, Belgium. Phone: +32 16 32 16 54, fax: +32 16 32 19 76, email: luc.schueremans@bwk.kuleuven.be

<sup>3</sup>PhD, Assistant Professor, ISISE, University of Minho, Department of Civil Engineering, Azurém, P-4800-058 Guimarães, Portugal. Phone: +351 253 510 247, fax: +351 253 510 217, email: danvco@civil.uminho.pt

<sup>4</sup>MSc student, Catholic University of Leuven, Department of Civil Engineering, P-3001, Heverlee, Belgium. Phone: +32 16 32 16 79, fax: +32 16 32 19 76, email: karolien.dekoning@gmail.com

<sup>5</sup>MSc student, Catholic University of Leuven, Department of Civil Engineering, P-3001, Heverlee, Belgium. Phone: +32 16 32 16 79, fax: +32 16 32 19 76, email: tine.gyssels@gmail.com

## 1. INTRODUCTION

Raw earth is one of the most ancient building materials, as is confirmed by archaeological evidence from millenarian cities that were built entirely with earth, such as Jericho (Israel), Çatal Huyuk (Turkey), Harappa (Pakistan), Akhlet-Aton (Egypt), Chan-Chan (Peru), Babylonia (Iraq) and Duheros (Spain) ([Lacouture \*et al.\* 2007](#)). Nowadays, building with earth is often the only feasible alternative for housing in most developing countries, while in developed countries this is an option that has fallen out of practice over the past century. Despite that, there is a large housing stock built from earth, widely distributed around the world (Delgado and Guerrero 2007, Jaquin *et al.* 2008) and comprises many monuments and buildings of acknowledged historic, cultural and architectural value (Jaquin *et al.* 2006). Moreover, these constructions are common in zones of significant seismic hazard (Blondet *et al.* 2003), which compromises their further existence and puts at risk the life of millions of people.

There are several known techniques for building with earth, although the most common and widespread are adobe masonry and rammed earth ([Houben and Guillaud 1994](#), [Minke 2006](#)). Adobes are moulded blocks of moistened earth that are sundried, while rammed earth consists of compacting layers of earth between formwork, whereby walls are erected. Nevertheless, earthen materials are non-industrial ([Bui \*et al.\* 2008](#)) and usually present great vulnerability against several damaging agents, such as earthquakes and floods (Houben and Guillaud 1994, Warren 1999). It is a fact that the seismic performance of earth constructions is, in general, poor, due to several factors ([Lacouture \*et al.\* 2007](#)), the very low tensile strength of earthen materials is probably the first to be noted. Despite that, the seismic performance of earth constructions relies on their monolithic behaviour rather than on the mechanical properties of earthen materials, so the good condition of the structural elements and of the connections granting their continuity is essential towards good seismic performance. The presence of cracks in load-bearing walls, besides constituting a path for further propagation of damage, greatly decreases the overall strength and stiffness of the construction, in which case they must be repaired in order to re-establish the original structural performance (Tolles *et al.* 1996). The repairing techniques usually employed (partial rebuilding, filling with mortar, stitching, etc.) often fail to establish continuity (bond), are excessively intrusive, or are of difficult execution (Warren 1999, Keefe 2005, [Silva \*et al.\* 2010](#)). In this context, grouting may constitute a repair solution that is more feasible, efficient and economic. Nevertheless, grouts compatible with earthen materials must be employed, which is not the case of those used for consolidating historic masonry

(fired clay brick or stone), including the recently developed binary and ternary grouts (Toumbakari 2002). The obvious trend is to adopt grouts incorporating earth, also called mud grouts (Warren 1999). A design methodology needs to be developed, although this has proven to be a difficult task. Besides the limited knowledge on these grouts, there are several problems arising, related to specific characteristics of earth as a repair material.

The experimental program presented in this paper was carried out with the purpose of studying and clarifying the influence of the mud grout composition, namely the clay content, on properties that govern the efficiency and applicability of a grouting intervention. The main focus was given to the rheological behaviour of fresh-state mud grouts, but the hardened-state strength and adhesion were also partly addressed. The aim is to complement the knowledge generated by previous works on mud grouts, which in general are more concerned with practical questions rather than trying to understand the problem itself.

## **2. BACKGROUND OF MUD GROUTS**

Currently, there are several published works on grouts for the consolidation of historical masonry ([Vintzileou and Tassios 1995](#), Toumbakari 2002 and [Vintzileou and Miltiadou-Fezans 2008](#)). However, there are only few cases where mud grouts are studied or applied for repairing earth constructions (Oliver 2008), and furthermore the information provided is, in general, limited. For example, Roselund (1990) describes a grouting solution applied to the restoration and strengthening of the Pio Pico mansion in Whittier, California, which is built in adobe. The damage to this mansion was mainly in the form of cracks in the adobe walls, as a consequence of the 1987 California earthquake. The cracks were repaired by injecting a modified mud grout (mud grout whose hardening relies not only on clay but also on another binder), whose composition consisted of earth, silica sand, fly ash and hydrated lime. The design of this mud grout was mainly focused on obtaining a material with adequate consistency, acceptable shrinkage, and with hardness, strength and abrasion resistance similar to those of the original adobes. The results of the preliminary study of the intervention project showed that the tested unmodified mud grouts presented excessive shrinkage, while the modified ones presented low shrinkage, justifying the preference for this latter type of grout. Later on, in 1994, the Pio Pico mansion was struck by the Northridge earthquake. The resulting minor to moderate damage, when compared to the damage to other buildings in a similar condition, showed that grout injection in combination with other consolidation/strengthening measures (strengthening of wall intersections with GFRP tie rods cored and grouted

into the walls, introduction of vertical anchors cored and grouted into the tops of gable-end walls and anchoring of the north wall to the south wall) were effective in preventing serious additional damage (Tolles *et al.* 1996).

Jäger and Fuchs (2008) also used grout injection for consolidating the remaining adobe walls of the Sistani House at Bam Citadel in Iran, severely damaged during the 2003 earthquake. A modified mud grout composed of clay powder, lime and wallpaper paste was employed for this purpose. The decision on the grout composition was preceded by a composition study that included testing the addition of other materials (such as cement and water glass). The shrinkage and the mechanical properties, namely the compressive, flexural and splitting tensile strengths, were the properties that were controlled.

On the other hand, Vargas *et al.* (2008) defends the employment of unmodified mud grouts rather than modified ones. This point of view is supported by an extended set of splitting tests carried out on specimens consisting of adobe sandwiches bonded by a layer of mud grout. Several compositions were tested, including unmodified and modified mud grouts (modified by the addition of different percentages of cement, lime or gypsum). Their results showed that, in general, the unmodified mud grouts have better adhesion capacity. In addition, the results of diagonal compression tests performed on adobe masonry wallets repaired by injection of an unmodified mud grout showed that it is possible to recover the initial strength of the damaged walls. Furthermore, the addition of binders, such as cement or hydraulic lime, greatly increases the Young's modulus of a mud grout, which may be from one to two orders of magnitude higher than that of earthen materials (On Yee 2009, [Silva et al. 2010](#)). Despite the advantages of modified mud grouts regarding shrinkage and resistance to water, its employment must be carefully evaluated, since excessive stiffness constitutes an important drawback with respect to satisfying mechanical compatibility with earthen materials.

The role of the construction and its interaction with hardened grout is another key point that is highlighted by Vargas *et al.* (2008), while other documents are mainly focused on the material properties of the grout. As is pointed out by [Silva et al. \(2009\)](#), the design of a mud grout is a complex process. In the first instance it must consider the demands of the construction, namely recovering structural behaviour and granting durability (see Fig. 1), in a similar approach to that used in the conservation of historical masonry (Toumbakari 2002). Then, the composition is defined such that the properties of the mud grout, namely the fresh-state rheological behaviour and stability and the hardened-state bond capacity, mechanical properties, chemical stability and

microstructure, meet the demands. All these properties have their particular role in the success of the grouting intervention, configuring to them similar importance. The complexity of the design of a mud grout resides however in the interdependence between these properties, which is specially exhibited when the composition is adjusted. Therefore, it is essential to understand how the composition of a mud grout affects its properties in order to design it effectively.

The rheological behaviour of fresh mud grouts has great importance on their injectability and, consequently, on their applicability and on the quality of the grouting intervention. The grout must feature adequate fluidity and penetrability in order to, in a first instance, allow it to be injected (applicability), and in a second instance, allow it to completely fill a crack and assure the continuity of the repaired earthen material (efficiency). On the other hand, both features depend on the texture of the solid phases (particles size distribution and shape), interaction between particles (dispersion or flocculation), solid fraction of the grout, mixing procedure and effect of dispersants/deflocculants. The clay fraction of a mud grout (i.e. the finer particles) is expected to have the main importance regarding to the rheological behaviour. The commoner plate-like shape of clay particles is an impediment to the flowing of the grout, because in the onset of the flow it tends to orientate the clay particles in the flow direction. However, it is the interaction between these small-sized particles (whereas a great percentage has colloid-size, i.e., dimension bellow 1  $\mu\text{m}$ ) that is expected to have the greatest impact. The mandatory high solid fraction of mud grouts promotes the collision between clay particles by reducing their average distance, which by its turn promotes their flocculation and consequently the reduction of fluidity of the mud grout. Moreover, and generally speaking, clay particles are characterized by a heterogeneous surface charge that under specific conditions promotes Face-to-Edge (FE) flocculation, responsible for a drastic reduction of the fluidity. Despite that, the manipulation of the surface charge or properties of the clay particles by addition of specific compounds (clay dispersants/deflocculants) is a solution usually applied to solve this problem, for example, in the ceramic and mining industry.

The drying shrinkage of a mud grout is a phenomenon that must be limited in order to grant the continuity disrupted by a crack, and thus to promote the good efficiency of the grouting intervention. This requires the adoption of high solid fractions that, as mentioned previously, limit the fluidity of the grout. Furthermore, the higher the clay content of an unmodified mud grout, the higher is the expected fluidity reduction. On the other hand, this fraction is essential towards the development adhesion and strength, as it constitutes the only binder. Therefore, the clay content is a feature that must be optimized to obtain adequate fluidity, drying shrinkage,

strength and adhesion. The understanding of how the composition does affect these properties is the aim of this paper for the case of unmodified mud grouts, whose importance is crucial towards the development of a design methodology. It should be mentioned that, the drying shrinkage of the studied mixes was not characterized in the paper, as it depends on external factors that are not easily simulated to provide reliable experimental results. In fact, the drying shrinkage of earthen materials is a complex problem requiring further research, which is out of the scope of the current paper.

### **3. EXPERIMENTAL PROGRAM**

#### **3.1 Materials**

With the aim of understanding the influence of the clay fraction (particle size below 2  $\mu\text{m}$ ) on the rheological behaviour of an unmodified mud grout in its fresh-state, several aqueous mixes were tested. The mechanical strength and adhesion capacity during the hardened-state were also evaluated for selected mixes. Instead of using natural soil for establishing the solid phase of the mixes, kaolin powder (Wienerberger, Kaolin RR40) and limestone powder (Carmeuse, Calcitec 2001 S) were used, which represent the clay and silt fractions of a mud grout, respectively (see Fig. 2). This procedure was preferred since the proportions between the solid fractions and the characteristics of these materials could be more easily controlled, more uniform and homogeneous throughout the experimental program than those of a natural soil. Furthermore, it was decided to use kaolin RR40 since this is a material mainly constituted of kaolinite (87%), a non-swelling clay mineral ([Van Olphen 1977](#)). The physical properties of both materials are given in Table 1. A deflocculant for clays, namely sodium hexametaphosphate (HMP), was also used in the composition study.

#### **3.2 Mixes and mixing procedure**

The composition study includes the testing of a total of 98 mixes of different materials in the solid phase, whereby they were grouped into the following types: kaolin (K); kaolin and HMP (KH); kaolin and limestone powder (KL); and kaolin, limestone powder and HMP (KLH). The variables of the study are then the volumetric solid fraction ( $\phi_v$ ), the amount of HMP added as function of the kaolin content ([HMP]) and the ratio between the weight of kaolin and limestone powder ( $K/L$ ). In Fig. 3, these variables are combined in order to present the tested compositions. Changing  $\phi_v$  of each mix type allows investigating the dependence of the rheological behaviour of the mixes on the solid content. This was expected to give an idea of the maximum  $\phi_v$  of each mix

type while obtaining a flowable behaviour that permits its injection at low pressure (for example, injection by gravity), which is defined by its capacity to flow or not through the Marsh cone. Regarding the importance of limiting the drying shrinkage of mud grouts, this is also an important finding. By altering the [HMP] it was expected to conclude about the capacity of this compound (or similar) in improving the fluidity of mud grouts. The variation of the clay content is reflected through the variation of  $K/L$  of the KLH mixes. With this, it was expected to conclude about the influence of the clay content in the rheological behaviour and strength of a mud grout.

The same mixing procedure was followed for all mixes. First, the solid phase materials were manually dry-mixed and then tap water (when HMP was added, it was first dissolved in the composition water) was progressively added and hand mixed until obtaining homogeneity. Afterwards, the mixes were mixed in three steps by a Hobart N50 planetary mixer with a wire whip paddle: first for 5 min at speed 1, then for 5 min at speed 2 and finally for 5 min at speed 1. In between each step, the mixes were left to rest for 1 min.

### **3.3 Experimental procedures**

#### *Rheology*

The flow time of each mix was determined according to the procedure of ASTM C 939 (1994), using a Marsh cone with an average flow time of 34 s for 1 dm<sup>3</sup> of water at 18°C and with the geometry of Fig. 4. All the tests were initiated within 1 min after the mixer being stopped, in order to minimize the interference of the possible time-dependent behaviour of the mixes on the results. The KH mixes that were apparently less fluid or that showed great difficulty in flowing through the Marsh cone (or did not flow at all) had, in addition, their flow curves determined by means of a Viskomat PC mixer-type rheometer (see Fig. 5) with a mortar paddle of 83 mm diameter (Hendrickx 2009). The flow profile applied is given in Fig. 6a. The flow curves of the KLH mixes were also determined, but by applying a different flow profile, given in Fig. 6b. Both profiles include an ascending stepwise branch followed by a descending stepwise branch in order to assign a similar reference state to all mixes. Moreover, this kind of flow profile also allows investigating the time-dependent behaviour. In each step it was recorded 7 to 8 data points, of which a trimmed average was taken. The rheological parameters were only computed for the descending branch.

#### *Strength*

The flexural and compressive strengths were tested for each KLH mix on three beam specimens with dimensions 40×40×160 mm<sup>3</sup>, according to EN 1015-11 (CEN 1999). It must be noted, however, that the age for testing the specimens was defined in such a way that the equilibrium water content (ratio between weight of water and weight of solid particles) could be established before testing, since the mechanical properties of earthen materials

greatly depend on it (Jaquin 2008). Therefore, the specimens were stored and dried in a controlled ambient room temperature ( $T= 20^{\circ}\text{C}$ ) and humidity ( $RH= 65\%$ ), and the evolution of their weight was monitored after demoulding (this was possible at ages 4 to 7 days). As it can be observed from Fig. 7a, the demoulded specimens achieve a constant weight in a short-time (3 to 5 days) which corresponds to the equilibrium water content. Thus, the beams were tested at ages ranging from 29 to 31 days, whereas the equilibrium water content was measured after testing, see Fig. 7b. For all mixes, this parameter is very low and it seems to depend mainly on the kaolin content, as stated in Johansen and Dunning (1957).

### *Adhesion*

The adhesion developed between earthen materials and three selected mixes (see Table 2) was tested on 18 earthen beams ( $160\times 40\times 40\text{ mm}^3$ ) built with three types of soil typically used in the construction of rammed earth houses in Alentejo (Portugal). Due to the small dimensions of the specimens, the soils were sieved in advance to remove particles larger than 2 mm, resulting in the physical properties given in Table 3. The preparation of the specimens consisted in compacting three layers of moistened earth within a typical metallic mould for mortars (see Fig. 8a), which were immediately demoulded and stored in a controlled ambient room temperature ( $T = 20^{\circ}\text{C}$ ) and humidity ( $RH = 65\%$ ). The water content for compaction was defined such that in the ball dropping test (Minke 2006) the ball would present some cracks without crumbling completely. The flexural strength of the beams was tested after 23 days (after achieving the equilibrium water content), according to the procedure of EN 1015-11 (CEN 1999). Afterwards, the beams were repaired by injecting the selected mixes (2 beams of each soil per mix) into the crack between the two parts of each beam (see Fig. 8b), which were positioned in a mould to provide an approximate crack width of 5 mm. Before injection, the faces of the beams contiguous to the crack were scraped and wetted, in order to eliminate loose material and mitigate the sorption of water from the mud grout. It should be mentioned that the drying and hardening of the grouts took only a few minutes, showing the high sorption capacity of earthen materials, which can be a drawback in an injection intervention due to a decrease in injectability. The repaired beams were stored in the aforementioned room, and were retested after 15 days.



## 4. RESULTS AND DISCUSSION

### 4.1 Rheology

The results of the flow time tests of the K mixes are presented in Fig. 9a, where it is observed that the higher the  $\phi_v$ , the higher the measured flow time. Moreover, for  $\phi_v$  between 9% and 10% a critical solid fraction ( $\phi_{vcr}$ ) is reached, after which flow through the Marsh's cone is no longer possible. This corresponds to a very low solid fraction, which is not suitable for a potential grout since it would result in high shrinkage (W/S between 3.8 and 3.4). On the other hand, adopting a larger  $\phi_v$  would result in a grout with inferior injectability properties, making its injection at low pressure rather difficult or impossible. This behaviour is a consequence of the colloidal behaviour of the kaolinite particles in suspension, which interact with each other under Brownian or/and hydrodynamic motion, generating two possible states of the particles: deflocculated or flocculated ([Van Olphen 1977](#)). The interaction between kaolinite particles is governed by DLVO (Derjaguin-Landau-Verwey-Overbeek) forces, namely electrostatic forces (repulsion between like electric double layers and attraction between unlike charged surfaces) and van der Waals attractive forces. In turn, the balance between these forces is dictated by several factors, such as the average distance between particles, their nature (permanent or variable) and the magnitude of the heterogeneous surface charge of the clay particles, the pH, and the ionic strength of the medium, etc. ([Tombácz and Szekeres 2006](#)). Therefore, when the attractive forces are favoured, the clay particles tend to flocculate, forming an internal structure (house-of-cards or scaffold structure) that opposes the flow. In the case of K mixes, the ionic strength of the medium is expected to be high, since tap water was used and the kaolin was not purified nor processed. This results in electric double layers at the kaolinite particles surfaces that are more collapsed, substantially decreasing the magnitude of the repulsion forces which are overcome by the van der Waals forces.

When HMP is added to the KH mixes, the following deflocculating mechanisms are expected: (i) increase in the overall negative surface charge by the adsorption of anionic HMP polymeric chains onto the kaolinite surface, especially at the edges of the kaolinite particles ([Andreola et al. 2006](#), [Legaly 2006](#)); (ii) stabilisation caused by the steric hindrance effect of the adsorbed HMP chains ([Papo et al. 2002](#)); (iii) complexing of the dissolved alkaline-earth cations and replacing them by lower valence  $\text{Na}^+$  cations, which increases the thickness of the electric double layers ([Andreola et al. 2006](#)). As can be seen in Fig. 9b, these mechanisms allow further increases in  $\phi_{vcr}$ , since it is possible to obtain flowing mixes until a  $\phi_v$  of 21% (W/S around 1.4). Moreover, the

higher the  $\phi_v$ , the higher the [HMP] required to decrease the flow time to its minimum, which in turn increases with  $\phi_v$ . On the other hand, the mixes incorporating higher HMP concentration had their flow time increased, which is explained by a concentration of linear polyphosphate chains that is above a critical value (saturation point) and that promotes the association of kaolinite particles instead of their repulsion (Papo *et al.* 2002).

The data obtained from the Viskomat PC rheometer was converted to shear rate and shear stress by means of Couette analogy. This method requires the determination of a fictitious radius  $R_i$  of a cylindrical bob, which would experience the same torque as that of the actual paddle. For a Newtonian fluid the ratio between the external radius  $R_e$  (0.042 m) and  $R_i$  is given by eq. (1)

$$\frac{R_e}{R_i} = \sqrt{1 + \frac{8\pi^2 L R_e^2 \mu 2\pi N}{T}} \quad (1)$$

Whereas,  $L$  (0.063 m) is the paddle length,  $\eta$  the viscosity of the fluid,  $N$  the rotation speed (in revolutions per unit of time) and  $T$  the recorded torque. This ratio was determined using a Newtonian fluid of known viscosity, and was found to be 1.154 (see Hendrickx 2009). The shear rate, viscosity and shear stress values at the middle of the fictitious gap can be approximately estimated from this radii ratio, according to:

$$\dot{\gamma} = \frac{2\pi N}{\ln\left(\frac{R_e}{R_i}\right)} \quad (2)$$

$$\mu = \frac{T}{2\pi N} \frac{\left(\frac{R_e}{R_i}\right)^2 - 1}{4\pi L R_e^2} \quad (3)$$

$$\tau = \mu \dot{\gamma} \quad (4)$$

It should be noted that in these equations it is assumed that the fluid is Newtonian, however Hendrickx (2009) shows that their application to cement and lime pastes (exhibiting Bingham behaviour within the tested range of shear rate) produces comparable results to those obtained from a Couette rheometer.

The action of HMP on the KH mixes is more thoroughly evidenced in Fig. 10a, where the shear stress required to shear the mixes decreases with increasing [HMP]. Moreover, the points of the descending branch of all KH mixes seem to exhibit Bingham behaviour, whereby the Bingham's law of eq. (5) was fitted to these points. This equation relates the shear stress ( $\tau$ ) with the shear rate ( $\dot{\gamma}$ ) by means of two parameters: yield stress ( $\tau_0$ ) and plastic viscosity ( $\mu_p$ ). In the cases that the fitting gave negative results for the yield stress, this parameter was forced to be 0 and the fitting was carried out again.

$$\tau = \tau_0 + \mu_p \dot{\gamma} \quad (5)$$

Both parameters are represented in Fig. 10b for the KH mixes with a  $\phi_v$  of 21%, where it is demonstrated that a little [HMP] is enough to reduce them substantially. The yield stress is related to the force required to deform and to disrupt the internal house-of-cards or scaffold structure previously mentioned. This type of internal structure is formed from the association between clay particles in edge-to-edge (EE) and edge-to-face (EF), in which the more numerous and as stronger these associations are, the higher the yield stress (Van Olphen 1977). The HMP added to the KH mixes is mainly adsorbed at the edge surfaces of the clay particles, which increases the magnitude of their negative surface charge, and thus reduces the frequency and strength magnitude of EE and EF associations. The reduction observed for the plastic viscosity is also a consequence of the effect of the HMP, since its addition allows a reduction in the number and size of flocks formed from the EE and EF associations, whereby less water is entrapped within them, decreasing the effective volumetric solid fraction ( $\phi'_v$ ) of the mixes with a higher [HMP] (Barnes *et al.* 1989). In the tested domain of rotation speeds, it is the yield stress that has the greatest contribution to the flowing resistance, and furthermore this parameter is the main responsible for the Marsh cone tests that failed. In these failed tests, the flow through the Marsh cone attained a critical situation before the cone is emptied, where the flow rate is zero. It should be noted that flow through the Marsh cone only occurs if the condition given by eq. (6) is observed:

$$\frac{2\tau_0}{Ar} \leq 1 \quad (6)$$

Where  $r$  is the nozzle radius and  $A$  the pressure gradient. For the complete flow of the Marsh cone, the pressure gradient assumes its minimum value at the nozzle and is written as follows:

$$A = \rho g \quad (7)$$

Where  $\rho$  is the density of the mix and  $g$  the gravitational acceleration. Considering that the density of the KH mixes varies from 1198 to 1347 kg/m<sup>3</sup>, the maximum yield stress that grants complete flow is calculated resorting to eq. (6) and ranges between 14 and 16 Pa.

Fig. 10b also demonstrates the effect of exceeding the critical HMP concentration, which results in an increase in both parameters. Another curious result is that the hysteresis observed in the results indicates an anti-thixotropic behaviour, which is contrary to the expected thixotropic behaviour usually reported. This is explained by the low shear rate range of the tests (when compared with the range of shear rate usually found in the bibliography), which is, most probably, promoting the association of clay particles, and thus the build-up of the aforementioned internal structure.

The results of the flow time tests of the KL mixes are presented in Fig. 11, that shows the effect of the clay fraction on fluidity. As the clay content increases ( $K/L$  increases) the flow time increases. Moreover, it is shown that by substituting the clay content with a silt size material (limestone powder), significantly increases  $\phi_{ver}$  when compared to the K and KH mixes.

Upon combining the effect of HMP with that of the incorporation of limestone powder, it is possible to further increase  $\phi_{ver}$ , since flowing suspensions with  $\phi_v$  from 55% to 60% (W/S between 0.3 and 0.25) were obtained, as shown in Fig. 12. However, the flow times increased substantially when compared with those of the K, KH and KL flowing mixes. Moreover, it should be noted that the results show a tendency that seems contrary to that of the KL mixes, in the sense that the mixes with lower  $K/L$  ratios have higher flow times. This is explained by the fact that [HMP] is a function of the kaolin content, whereby the effective HMP content in mixes with lower  $K/L$  is also lower. In addition, it is expected that HMP also has a deflocculating/dispersing effect on the limestone powder, as it is shown in Fig. 13, whereas the flow time of the limestone powder and HMP mixes (LH mixes) with a  $\phi_v$  of 50% is given as function of the ratio between the weight of HMP and the weight of limestone powder ([HMP]<sup>2</sup>).

As can be seen in Fig. 14, the KLH mixes also seem to exhibit Bingham's behaviour, whereby the Bingham's parameters were computed in the same way as those computed for the KH mixes. Some KLH mixes also exhibit

anti-thixotropic behaviour, which revealed tendency to be extensively attenuated with the addition of higher percentages of HMP. In terms of Bingham's parameters, it is shown that HMP has greater impact on the reduction of the yield stress than it has on the plastic viscosity (see Fig. 15). In fact the addition of higher quantities of HMP brings the yield stress to values close to zero, which is an important finding regarding the success of a grouting intervention ([Brás and Henriques 2012](#)). This importance resides in the fact that if the injection pressure of a mud grout into a crack is not sufficient to keep the shear stress at the head higher than the yield stress the flow stops. Such situation impedes the complete filling of the crack by the grout. This is an identical circumstance to that of the failed Marsh cone tests, where the flow of the KLH mixes (density between 1931 and 2019 kg/m<sup>3</sup>) according to Eq. (6) would not occur completely for yield stresses greater than 23 to 24 Pa. On the other hand, the plastic viscosity values obtained from the KLH mixes are substantially higher than those obtained from the KH mixes, as result of the substantially higher  $\phi_v$  of the KLH mixes. This explains the higher flow times measured in these mixes.

The limitations of the Marsh cone as a rheological apparatus are known; however Le [Roy and Roussel \(2005\)](#) proposed the expression of Eq. (8) that allows computing the flow time ( $t_V$ ) as function of the geometry of the cone, assuming that the fluid is Newtonian.

$$\begin{aligned}
 t_V = & \frac{8\mu}{3\rho gr^3 \tan(\alpha)} \left( \left(1 + \frac{3h \tan(\alpha)}{r}\right) (\tan^2(\alpha)(H_0 - H) \left(\frac{H_0 - H}{2} + h\right) \right. \\
 & - 2 \tan(\alpha)(h \tan(\alpha) - r)(H_0 - H) + (h \tan(\alpha) - r)^2 \ln\left(\frac{H_0 + h}{H + h}\right) \right) \\
 & - \frac{r^3}{h \tan(\alpha) - r} \left( \ln \frac{H_0 \tan(\alpha) + r}{H \tan(\alpha) + r} - \ln\left(\frac{H_0 + h}{H + h}\right) \right)
 \end{aligned} \tag{8}$$

Where, the geometrical parameters of the Marsh cone are given in Fig. 4. Since the tested flow times are relative to the complete flow of the material,  $H$  is considered to be zero. Later on Roussel and Le Roy (2005) proposed Eq. (9), where the fluid is assumed to have Bingham's behaviour. The parameter  $a_V$  is given by Eq. (10), where  $V$  is the tested volume, while  $b_V$  is given by Eq. (11).

$$t_V = \frac{a_V \mu_p}{\rho - b_V \tau_0} \tag{9}$$

$$a_v = \frac{8V \tan(\alpha)(3h(H_0 \tan(\alpha) + r)^3 + H_0 r(H_0^2 \tan^2(\alpha) + 3H_0 r \tan(\alpha) + 3r^2))}{(3\pi r^3 \tan(\alpha) gr(h + H_0))(H_0 \tan(\alpha) + r)^3} \quad (10)$$

$$b_v = \frac{\pi r^3 (8r \ln(H_0 \tan(\alpha) + r) - 8r \ln(r) + 8h \tan(\alpha))}{3\pi r^3 \tan(\alpha) gr(h + H_0)} \quad (11)$$

Eq. (8) and Eq. (9) were used to predict the flow time of the KLH with base on the parameters obtained from the flow curves. The predicted flow times were plotted against the measured flow times in Fig. 16, where can be seen that both equations give reasonable approximation of the flow time. From the application of Eq. (9) resulted a low average error, which is rather satisfactory since the development of this equation considers the flow constant, which is only valid for the first half of the test Roussel and Le Roy (2005).

## 4.2 Strength

The flexural strength of the KLH mixes with K/L of 0.15 is presented as function of  $\phi_v$  in Fig. 17a. It appears that there is no relation between these parameters with the exception of the mixes with an [HMP] of 20g/kg. On the other hand, the compressive strength of the mixes seems to be favoured by an increasing  $\phi_v$  (see Fig. 17b).

In regard to the effect of clay content, the increase of K/L in the KLH mixes promoted a positive development of both strength parameters (see Fig. 18). Moreover, the mixes with a low K/L developed flexural and compressive strengths that are quite satisfactory when compared with those of earthen materials (see Table 4), and thus gives an indication that reducing the clay content to very low values for favouring the rheological behaviour of a mud grout does not have undesirable consequences on its strength. However, the generalization of this remark must be regarded carefully, since the binding capacity of the clay in an earthen material also depends on its properties, such as clay minerals, particle size distribution and surface area. In addition, lowering the clay content decreases the water resistance of the earthen material and thus its durability (Minke 2006).

## 4.3 Adhesion

The results of the three-point bending tests performed on the repaired earthen beams, as well as the repair efficiency of the selected mud grouts, are presented in Fig. 19. The grouts failed at re-establishing the original strength of the earthen beams. However, the repaired beams developed a flexural strength of at least 0.5 N/mm<sup>2</sup>,

which is above the minimum flexural strength for adobes required by the New Mexico (NMAC 2006) and New Zealand (SNZ 1998) standards, of 0.35 and 0.25 N/mm<sup>2</sup> respectively.

The soils used to prepare the beams were previously sieved, which results in a higher clay content and, thus, in higher flexural strength than potentially that of a rammed earth block built with unsieved soil. Therefore, the efficiency of these mud grouts on such hypothetical blocks is expected to be greater than on earthen beams.

The  $\phi_v$  of the selected grouts does not seem to interfere significantly with the repair efficiency, which probably means that the water content of the mud grout may be further increased in order to favour its injectability properties, accounting, however, for the possibility of excessive drying shrinkage occurring.

Regarding the failure mode of the repaired beams, most of them failed along the grout (see Fig. 20a), nevertheless for some beams of soil S3, failure at the grout-beam interface was also observed (see Fig. 20b). These failure modes are preferable to the failure of the earthen beam, since the integrity of the original earthen material is preserved.

## 5. CONCLUSIONS

The composition study presented and discussed in this paper allows clarification of the influence of the composition of an unmodified mud grout on three of the most important properties that govern the application and efficiency of a grouting intervention on an earth construction, namely rheology, strength and adhesion.

The composition study performed indicates that the clay fraction has great influence on the rheological behaviour of an unmodified mud grout. Increasing the  $\phi_v$  of an aqueous mix of clay promotes the flocculation of clay particles which is responsible for the formation of an internal house-of-cards or scaffold structure. The flow through the Marsh's cone is hindered for  $\phi_v$  higher than  $\phi_{ver}$ . The addition of a deflocculant, such as HMP, promotes the repulsion between clay particles, which allows further increase in  $\phi_{ver}$  of the KH mixes when compared to that of the K mixes. The flow curves determined for the KH mixes showed that increasing amounts of HMP decrease the resistance to flow by means of reduction of the Bingham parameters, which is a consequence of the weakening and disruption of the internal structure. Adding increasing amounts of silt size

materials (such as limestone powder), for decreasing the clay content of the mix, also results in a further increase of  $\phi_{ver}$ .

However, designing a mud grout with adequate  $\phi_v$  (to avoid excessive drying shrinkage) demands accounting for the previous two effects as was shown by the results obtained for the KLH mixes, where it was possible to obtain flowing mixes with  $\phi_v=60\%$ . On the other hand, the measured flow time of these mixes was revealed to be very high, as consequence of the high values obtained for the plastic viscosity. The addition of HMP was mainly reflected in the reduction of the yield stress to values close to zero, which may be an important feature if a mud grout is to be injected at low pressure.

Regarding the strength of unmodified mud grouts, it was shown that the higher the clay content, the higher the flexural and the compressive strength. Nevertheless, the maximum clay content of a mud grout must be limited, since excessive clay content has negative impact on its rheological behaviour. A compromise should be found between these properties.

The adhesion capacity of the KLH mixes selected allowed substantial recovery of the original strength of the earthen beams tested, where the minimum flexural strength obtained was greater than  $0.5 \text{ N/mm}^2$ . Moreover, the range of  $\phi_v$  tested seemed to have no interference on the efficiency of the repair, which means that  $\phi_v$  may be lowered for favouring the rheological behaviour. Further research must be done regarding the adhesion of mud grouts, namely their application on larger specimens, and the evaluation of their shrinkage magnitude and mode.

Finally, it should be noted that the generalisation of the results presented in this paper should be considered carefully, especially with regards to the rheological behaviour, since the magnitude of the phenomena discussed depends significantly on the properties of the clay fraction composing the mud grout.

## **ACKNOWLEDGEMENTS**

The authors wish to express their gratitude to the Portuguese Science and Technology Foundation for the scholarship granted to the first author (SFRH/BD/39145/2007) and to the company Wienerberger (Belgium) for kindly providing the kaolin.



## REFERENCES

- [Andreola, F., Castellini, E., Ferreira, J.M.F., Olhero, S. and Romagnoli, M. \(2006\) Effect of sodium hexametaphosphate and ageing on the rheological behaviour of kaolin dispersions, Applied Clay Science, 31, pp. 56-64.](#)
- [ASTM \(1998\) ASTM D 422-63: Standard test method for particle size analysis of soils, American Society for Testing and Materials, West Conshohocken, PA.](#)
- [ASTM \(1994\) ASTM C 939-94: Standard test method for flow of grout for preplaced-aggregate concrete \(flow cone method, American Society for Testing and Materials, West Conshohocken, PA.](#)
- [ASTM \(2000\) ASTM D 4318-00: Standard test method for liquid limit, plastic limit and plasticity index of soils, American Society for Testing and Materials, West Conshohocken, PA.](#)
- [Barnes, H. A., Hutton, J. F. and Walters, K. \(1989\) An Introduction to Rheology, Rheology Series Vol. 3, Elsevier, Amsterdam.](#)
- [Blondet, M., Garcia, G. and Brzev, S. \(2003\) Earthquake-Resistant Construction of Adobe Buildings: A Tutorial, Earthquake Engineering Research Institute, Oakland, California.](#)
- [Brás, A. and Heriques, F.M.A. \(2012\) Natural hydraulic lime based grouts – The selection of grout injection parameters for masonry consolidation. Construction and Building Materials, 26, pp. 135-144.](#)
- [Bui, Q.-B., Morel, J.-C., Hans, S. and Meunier, N. \(2008\) Compression behaviour of non-industrial materials in civil engineering by three scale experiments: the case of rammed earth, Materials and Structures, 42\(8\), pp. 1101-1116.](#)
- [CEN \(1999\) EN 1015-11: 1999: Methods of test for mortar for masonry – Part 11: Determination of flexural and compressive strength of hardened mortar, European Committee for Standardization, Brussels.](#)
- [CYTED \(1995\) Recomendaciones para la elaboración de normas técnicas de edificaciones de adobe, tapial, ladrillos y bloques de suelo-cemento. Sistematización del uso de la tierra en viviendas de interés social. Red Temática XIV.A HABITERRA-CYTED, Ottazzi, P., Martins, C., Vargas, N., Ribas, J., San Bartolomé, A. and de Silva, S.](#)
- [Delgado, M. and Guerrero, I. \(2007\) The selection of soils for unstabilised earth building: A normative review, Construction and building materials, 21\(2\), pp. 237-351.](#)
- [Hendrickx, R. \(2009\) The Adequate Measurement of the Workability of Masonry Mortar, PhD Thesis, Katholieke Universiteit Leuven, Leuven, Belgium.](#)

- Houben, H. and Guillaud, H. (1994) *Earth Construction: A Comprehensive Guide*, Intermediate Technology Development Group, London, England.
- Jäger, W. and Fuchs, C. (2008) Reconstruction of the Sistani House at Bam Citadel after the collapse due to the earthquake 2003, In: D' Ayala, D. and Fodde, E. (Eds.) *Preserving Safety and Significance*, Proceedings of the VI International Conference on Structural Analysis of Historic Constructions 2008, Vol. 2, Bath, UK, pp. 1181-1187.
- Jaquin, P.A. (2008) *Analysis of Historic Rammed Earth Construction*, PhD Thesis, Durham University, Durham, United Kingdom.
- Jaquin, P.A., Augarde, C.E. and Gerrard, C.M. (2006) Analysis of Historic Rammed Earth construction, In: Lourenço, P.B., Roca, P., Modena, C. and Agrawal, S. (Eds.) *Proceedings of the 5th International Conference on Structural Analysis of Historical Constructions*, New Delhi, India, pp. 1091-1098.
- Jaquin, P.A., Augarde, C.E. and Gerrard, C.M. (2008) Chronological Description of the Spatial Development of Rammed Earth Techniques, International Journal of Architectural Heritage, 2(4), pp. 377-400.
- Johansen, R.T. and Dunning, H.N. (1957) Water-vapor adsorption on clays, Clays and clay minerals, 6(1), pp. 249-258.
- Keefe L. (2005) *Earth Building: Methods and Materials, Repair and Conservation*, Taylor & Francis, London and New York.
- Lacouture, L., Bernal, C., Ortiz, J. and Valencia, D. (2007) Estudios de vulnerabilidad sísmica, rehabilitación y refuerzo de casas en adobe y tapia pisada, Apuntes, 20(2), pp. 286-303.
- Lagaly, G. (2006) Colloid clay science, In: Bergaya, F., Theng, B.K.G. and Lagaly, G. (Eds.) *Developments in Clay Science: Handbook of Clay Science*, Elsevier, The Netherlands, pp. 141-245.
- Le Roy, R. and Roussel N. (2005) The Marsh cone as viscometer: theoretical analysis and practical limits. Materials and Structures, 38 (1), pp. 25-30.
- Minke, G. (2006) *Building with earth: design and technology of a sustainable architecture*. Birkhäuser, Basel.
- NMAC (2006) NMAC 14.7.4: Housing and Construction: Building Codes General: New Mexico Earthen Building Materials Code, New Mexico Regulation and Licensing Department, Santa Fe, New Mexico.
- Oliver, A. (2008) Conservations of nondecorated earthen materials, In: Avrami E., Guillaud H. and Hardy M. (Eds.) *Terra Literature Review: An overview of research in earthen architecture conservation*, The Getty Conservation Institute, Los Angeles, pp. 108-123.

- On Yee, L. (2009) Study of earth-grout mixtures for rehabilitation, MSc Thesis, University of Minho, Guimarães, Portugal.
- Papo, A., Piani, L. and Riceceri, R. (2002) Sodium tripolyphosphate and polyphosphate as dispersing agents for kaolin suspensions: rheological characterization, *Colloids and Surfaces A: Physicochemical and Engineering Aspects*, 201, pp. 219-230.
- Roselund, N. (1990) Repair of cracked walls by injection of modified mud. In: Proceedings of the 6<sup>th</sup> International Conference on the Conservation of Earthen Architecture: Adobe 90 Preprints, Las Cruces, New Mexico, pp. 336-341.
- Roussel, N. and Le Roy, R. (2005) The Marsh cone: a test or a rheological apparatus?. *Cement and Concrete Research*, 35, pp. 823-830.
- Silva, R.A., Schueremans, L. and Oliveira, D.V. (2009) Grouting as a repair/strengthening solution for earth constructions. In: Proceedings of the 1st WTA International PhD Symposium, WTA publications, Leuven, pp. 517-535.
- Silva, R.A., Schueremans, L. and Oliveira, D.V. (2010) Repair of earth masonry by means of grouting: importance of clay in the rheology of a mud grout. In: Proceedings of the 8th International Masonry Conference 2010, Dresden, Germany, pp. 403-412.
- SNZ (1998). *New Zealand Standard 4298: 1998, Materials and workmanship for earth buildings*,: Standards New Zealand, Wellington.
- Tolles, E.L., Webster F.A., Crosby A. and Kimbro E.E. (1996) *Survey of Damage to Historic Adobe Buildings after the January 1994 Northridge Earthquake. The Getty Conservation Institute Scientific Program Report, Los Angeles.*
- Tombácz, E. and Szekeres, M. (2006) Surface charge heterogeneity of kaolinite in aqueous suspension in comparison with montmorillonite, *Applied Clay Science*, 34, pp. 105-124.
- Toumbakari E. (2002) *Lime-Pozzolan-Cement Grouts and their Structural Effects on Composite Masonry Walls. PhD Thesis, Katholieke Universiteit Leuven, Leuven, Belgium.*
- Van Olphen, H. (1977) Clay colloid chemistry: for clay technologists, geologists, and soil scientists, 2nd ed., Wiley-Interscience, New York.
- Vargas J., Blondet M., Cancino C., Ginocchio F., Iwaki C. and Morales K. (2008) Experimental results on the use of mud-based grouts to repair seismic cracks on adobe walls. In: D'Ayala D. and Fodde E. (Eds.)

Preserving Safety and Significance, Proceedings of the VI International Conference on Structural Analysis of Historic Constructions 2008, Bath, UK, pp. 1095-1099.

Vintzileou E., Miltiadou-Fezans A. (2008) Mechanical properties of three-leaf stone masonry grouted with ternary or hydraulic lime-based grouts, Engineering Structures, 30(8), pp. 2265-2276.

Vintzileou E., Tassios T.P. (1995) Three-leaf stone masonry strengthened by injecting cement grouts, Journal of Structural Engineering, 121(5), pp. 848-856.

Walker, P. and Standards Australia (2002) HB 195 – The Australian earth building handbook. Standards Australia, Australia.

Warren, J. (1999) Conservation of Earth Structures, Butterworth Heinemann, London.

## LIST OF TABLE CAPTIONS

Table 1 – Physical properties of the materials composing the solid fraction of the mixes.

Table 2 – Composition of the mud grouts selected for testing the bond with earthen materials.

Table 3 – Physical properties of the soils used in the bond test after being sieved.

Table 1 – Physical properties of the materials composing the solid fraction of the mixes.

| Material        | % Clay | % Silt | % Sand | Specific gravity (G) | PL (%) | LL (%) |
|-----------------|--------|--------|--------|----------------------|--------|--------|
| Kaolin RR40     | 81     | 10     | 9      | 2.65                 | 31     | 108    |
| Calcitec 2001 S | 6      | 65     | 29     | 2.71                 | -      | -      |

Clay: <0.002 mm / silt: ≥0.002 mm and <0.060 mm / sand: ≥0.060 mm and <2.0 mm (ASTM D 422-63 (ASTM 1964))

PL: Atterberg's plastic limit / LL: Atterberg's liquid limit (ASTM D 4318-00 (ASTM 2000))

Table 2 – Composition of the mud grouts selected for testing the bond with earthen materials.

| Mud Grout | $\phi_v$ (%) | [HMP] (g/kg) | $K/L$ | $W/S$ (wt.) |
|-----------|--------------|--------------|-------|-------------|
| MG_55     | 55           | 20           | 0.15  | 0.30        |
| MG_58     | 58           | 20           | 0.15  | 0.27        |
| MG_60     | 60           | 20           | 0.15  | 0.25        |

Table 3 – Physical properties of the soils used in the bond test after being sieved.

| Soil | % Clay | % Silt | % Sand | PL | LL |
|------|--------|--------|--------|----|----|
| S1   | 19     | 47     | 34     | 28 | 44 |
| S2   | 15     | 37     | 48     | 17 | 32 |
| S3   | 18     | 29     | 53     | 20 | 35 |

Clay: <0.002 mm / silt:  $\geq 0.002$  mm and <0.060 mm / sand:  $\geq 0.060$  mm and <2.0 mm (ASTM D 422-63 (ASTM 1964))

PL: Atterberg's plastic limit / LL: Atterberg's liquid limit (ASTM D 4318-00 (ASTM 2000))



Table 4 – Minimum compressive strength of earthen materials according to standards/recommendations.

| Standard/recommendation                  | Country        | Wall type                 | Compressive strength<br>(N/mm <sup>2</sup> ) |
|--|----------------|---------------------------|--|
| Walker and Standards<br>Australia (2002) | Australia      | Adobe                     | ≥1 <sup>a</sup>                              |
|  |                | Rammed earth              | ≥2 <sup>a</sup>                              |
| CYTED (1995)                             | -              | Adobe <sup>b</sup>        | ≥1.2 in 80% of the specimens <sup>c</sup>    |
|  |                | Rammed earth <sup>d</sup> | ≥1.2 in 80% of the specimens <sup>c</sup>    |
| NMAC (2006)                              | USA            | Adobe <sup>e</sup>        | ≥2.1   |
|  |                | Rammed earth <sup>f</sup> | >2.1   |
| SNZ (1998)                               | New<br>Zealand | Adobe <sup>g</sup>        | >1.3 <sup>h</sup>                            |
|  |                | Rammed earth <sup>i</sup> | >1.3 <sup>h</sup>                            |

Notes:

<sup>a</sup> dry unconfined characteristic strength obtained from earth blocks or cylindrical earth specimens. Aspect ratio correction factor must be applied.

<sup>b</sup> test on cubic specimens obtained from cutting an adobe.

<sup>c</sup> Characteristic compressive strength.

<sup>d</sup> 0.1 m sided cubic specimens.

<sup>e</sup> adobe in flat position.

<sup>f</sup> on cured rammed earth specimens. No info is provided on the specimens preparation.

<sup>g</sup> height/thickness=1 or aspect ratio correction must be applied.

<sup>h</sup> lowest of 5 specimens.

<sup>i</sup> in cured rammed earth specimens. No info is provided on the specimens preparation.

## LIST OF FIGURE CAPTIONS

Fig. 1 – Design methodology of a mud grout.

Fig. 2 – Particles size distribution curves of the kaolin and limestone powder (ASTM D 422-63) .

Fig. 3 – Matrix of the tested mixes composition.

Fig. 4 – Marsh's cone used in the tests (dimensions in mm).

Fig. 5 – Viskomat PC rheometer used for determining the flow curves of the mixes.

Fig. 6 – Viskomat PC flow profiles for (a) KH mixes and (b) KLH mixes.

Fig. 7 – Water content of the beam-specimens: (a) time evolution of the weight of KLH beams and (b) equilibrium water content.

Fig. 8 – Preparation of the earthen beams for (a) the adhesion tests and (b) injection of the earthen beams after testing.

Fig. 9 – Flow time measurements of (a) the K mixes and (b) the KH mixes.

Fig. 10 – Flow curves of (a) KH mixes with  $\phi_i=15\%$  (with Bingham's model fitted to the descending branch) and (b) Bingham's parameters of KH mixes with  $\phi_i=21\%$ .

Fig. 11 – Flow time measurements of the KL mixes.

Fig. 12 – Flow time measurements of the KLH mixes with  $\phi_i=55\%$ .

Fig. 13 – Flow time measurements of the LH mixes with  $\phi_i=50\%$ .

Fig. 14 – Flow curves of the KLH mixes with  $\phi_i=55\%$  and  $K/L=0.05$  (with Bingham's model fitted to the descending branch).

Fig. 15 – Bingham's parameters of KLH mixes with  $\phi_i=55\%$ .

Fig. 16 – Strength of the KLH mixes with  $K/L=0.15$ : (a) flexural strength and (b) compressive strength.

Fig. 17 – Strength of the KLH mixes with  $\phi_i=58\%$ : (a) flexural strength and (b) compressive strength.

Fig. 18 – Repair efficiency of the selected mud grouts for the three soil types.

Fig. 19 – Failure mode of the repaired earthen beams: (a) failure of the grout and (b) failure of the grout-earthen beam interface.

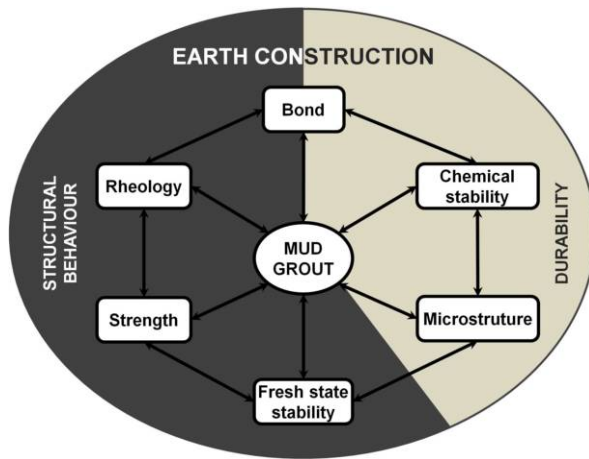


Fig. 1 – Design methodology of a mud grout.

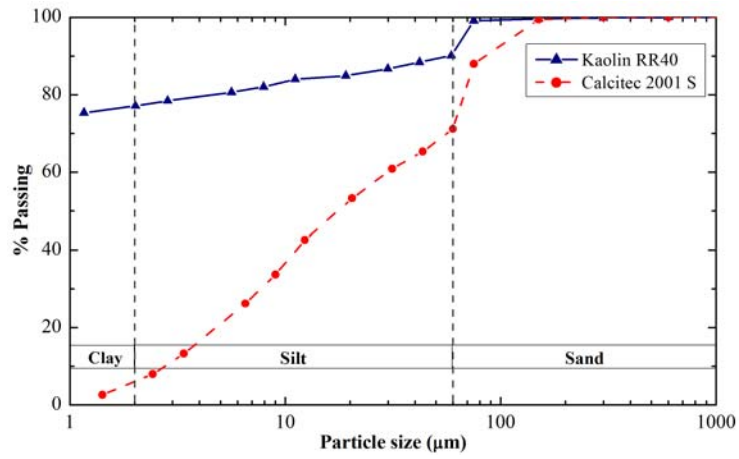


Fig. 2 – Particles size distribution curves of the kaolin and limestone powder (ASTM D 422-63).

| Mix Type      | K  | KH   | KL                         | KLH                   |
|---------------|--|--|----------------------------|-----------------------|
| $\phi_v$ (%)  | [4.0 5.0 6.0]<br>[7.0 8.0 9.0]<br>[10.0] | [9.0 12.0]<br>[15.0 18.0]<br>[21.0]            | [20.0 30.0]                | [55.0 58.0]<br>[60.0] |
| [HMP] (g/kg)* |  | [1.4 2.9 4.3]<br>[5.8 7.2 8.7]<br>[14.5 40 60] |                            | [5 10 15 20]          |
| $K/L$         |  |  | [0.2 0.3 0.4]<br>[0.5 0.6] | [0.05 0.10]<br>[0.15] |

\* weight (g) of HMP / weight (kg) of kaolin

Fig. 3 – Matrix of the tested mixes composition.

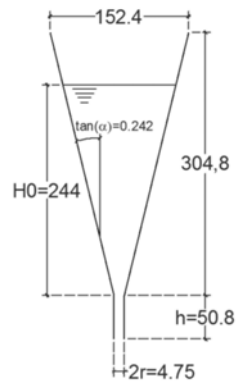


Fig. 4 – Marsh's cone used in the tests (dimensions in mm).



Fig. 5 – Viskomat PC rheometer used for determining the flow curves of the mixes.

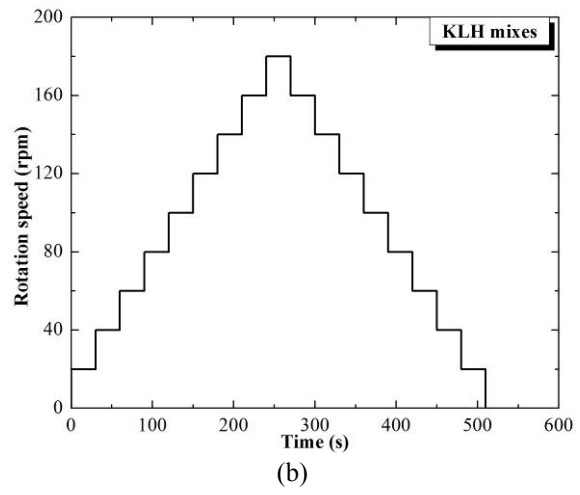
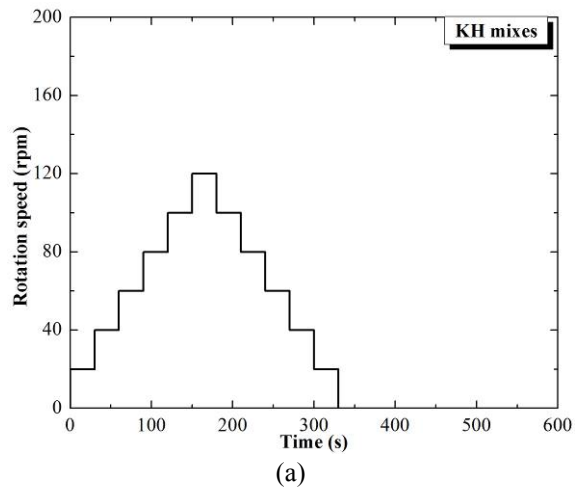


Fig. 6 – Viskomat PC flow profiles for (a) KH mixes and (b) KLH mixes.



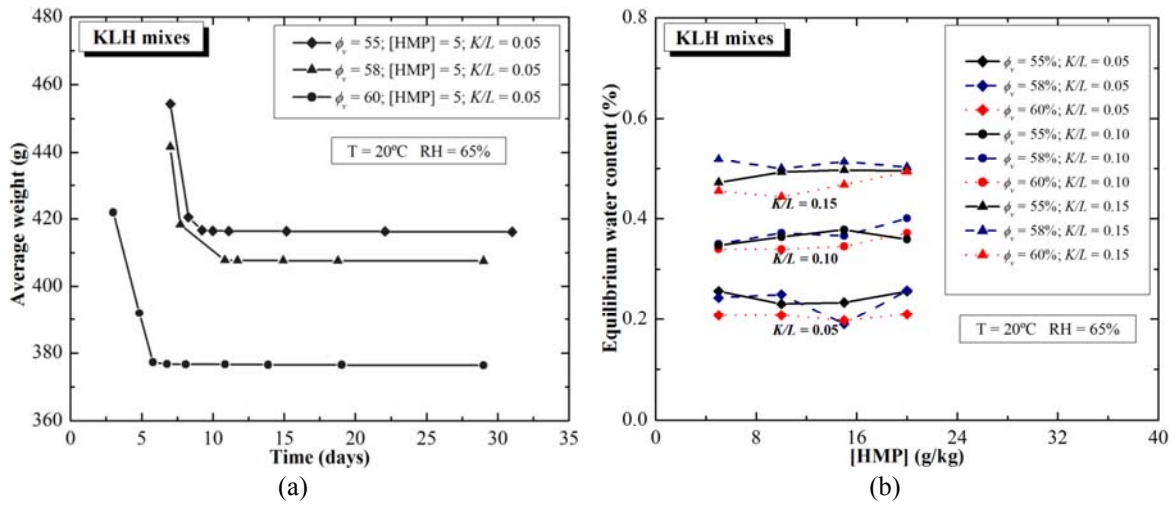
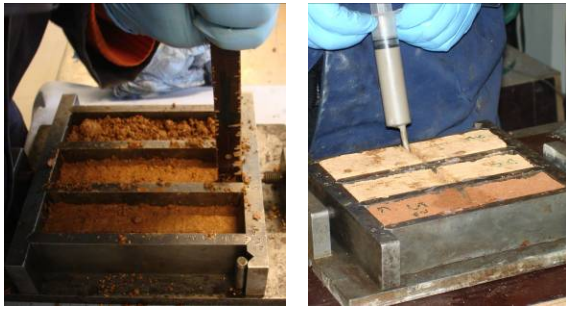


Fig. 7 – Water content of the beam-specimens: (a) time evolution of the weight of KLH beams and (b) equilibrium water content.



(a)

(b)

Fig. 8 – Preparation of the earthen beams for (a) the adhesion tests and (b) injection of the earthen beams after testing.

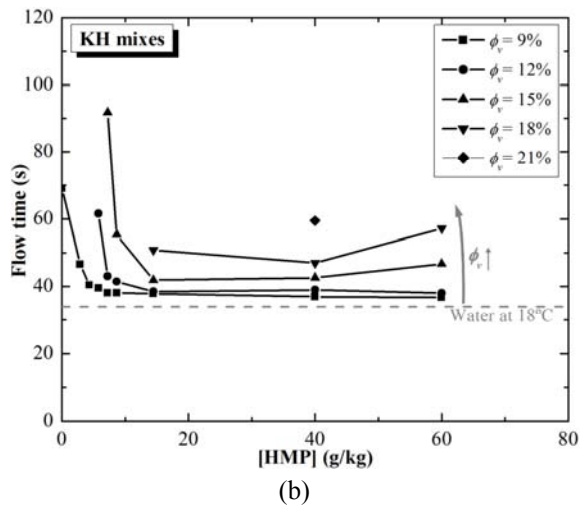
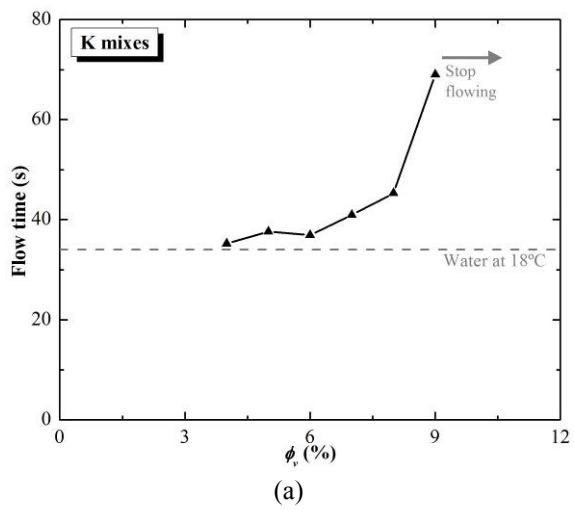


Fig. 9 – Flow time measurements of (a) the K mixes and (b) the KH mixes.

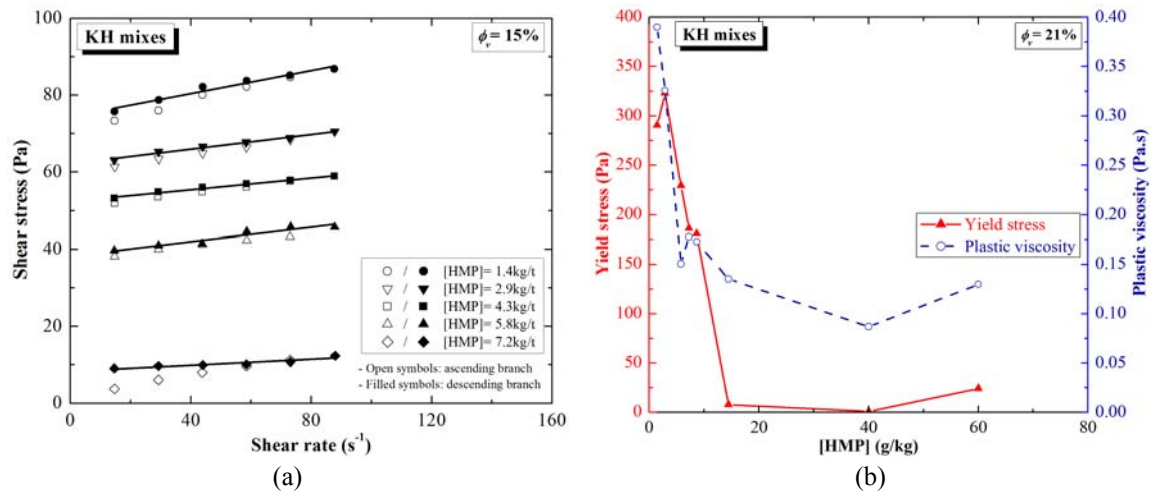


Fig. 10 – Flow curves of (a) KH mixes with  $\phi_v=15\%$  (with Bingham's model fitted to the descending branch) and (b) Bingham's parameters of KH mixes with  $\phi_v=21\%$ .

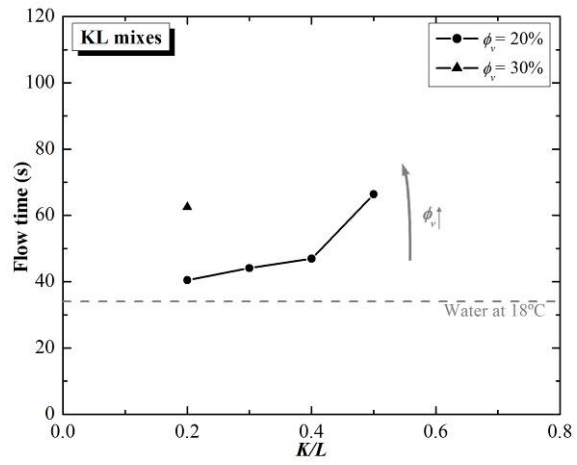


Fig. 11 – Flow time measurements of the KL mixes.

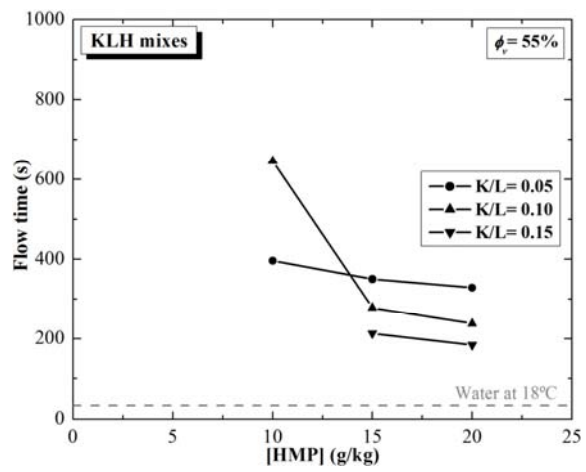


Fig. 12 – Flow time measurements of the KLH mixes with  $\phi_v=55\%$ .

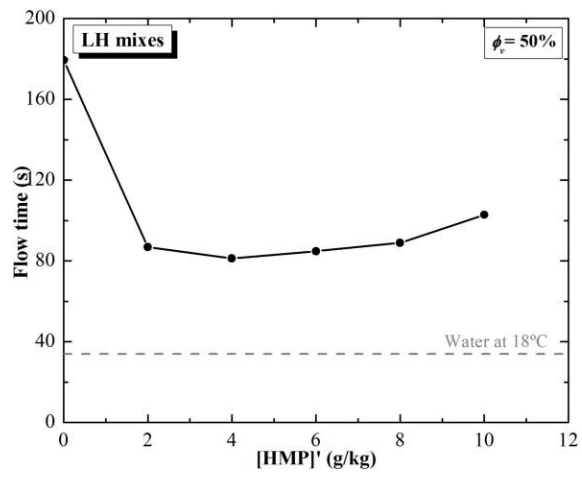


Fig. 13 – Flow time measurements of the LH mixes with  $\phi_v=50\%$ .

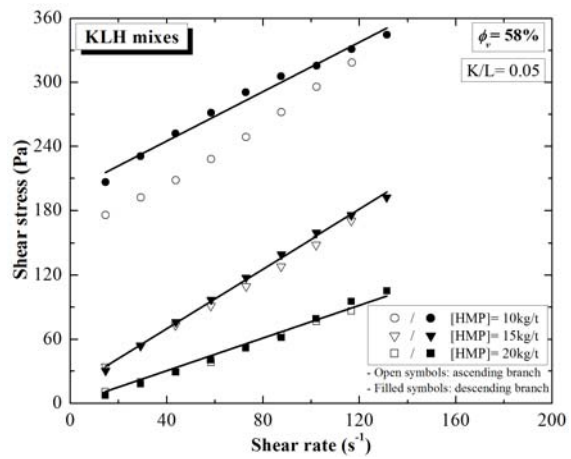


Fig. 14 – Flow curves of the KLH mixes with  $\phi_v=55\%$  and  $K/L=0.05$  (with Bingham's model fitted to the descending branch).



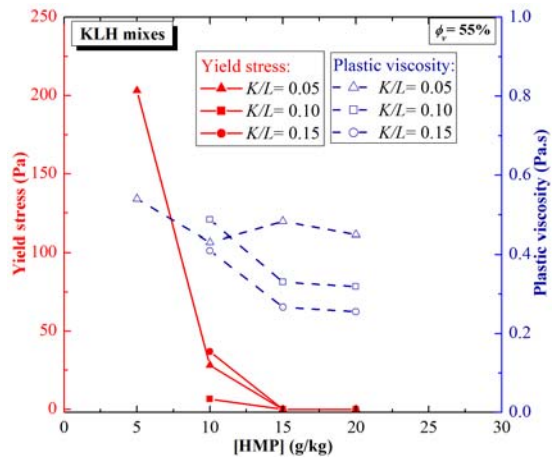


Fig. 15 – Bingham's parameters of KLH mixes with  $\phi_v=55\%$ .

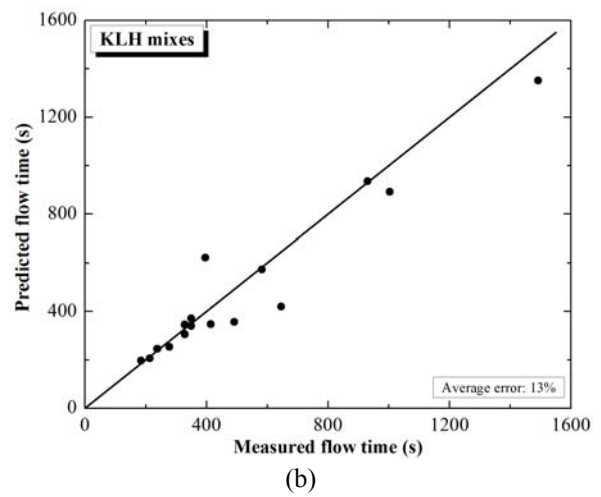
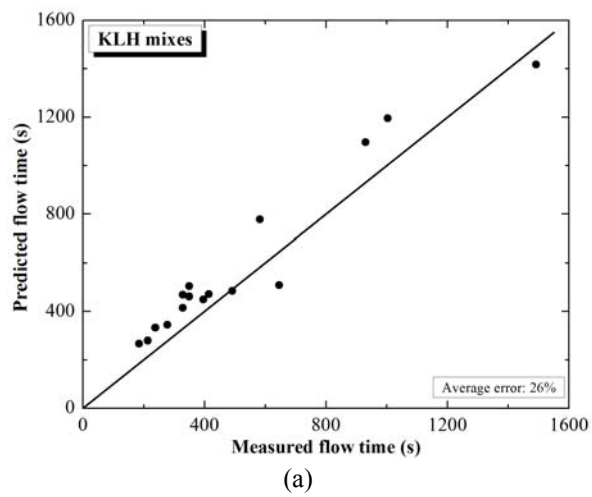


Fig. 16 – Comparison between the measure flow time and the predicted flow time using (a) Eq. (8) and (b) Eq. (9). The  $y=x$  curve is also plotted.

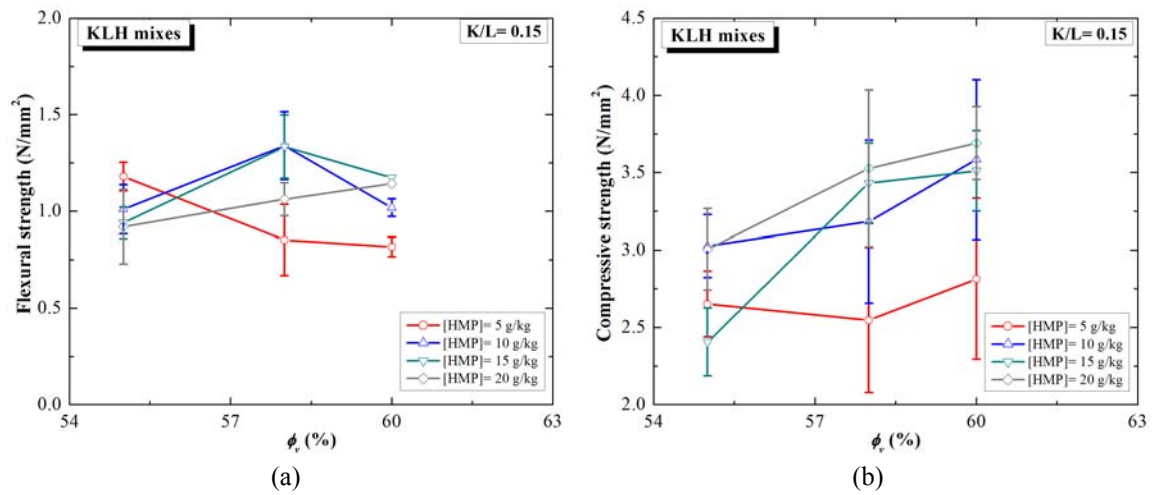


Fig. 17 – Strength of the KLH mixes with K/L=0.15: (a) flexural strength and (b) compressive strength.

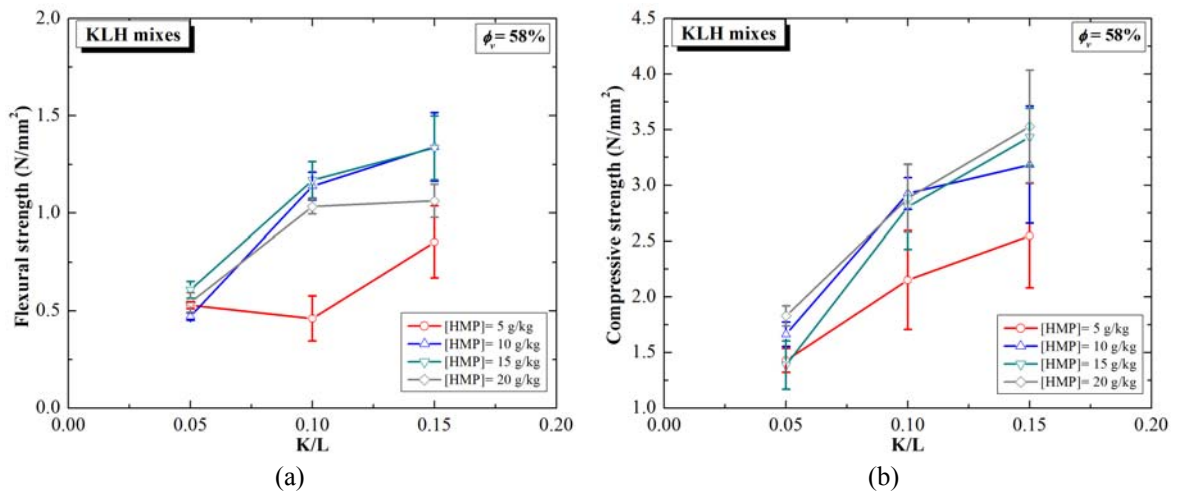


Fig. 18 – Strength of the KLH mixes with  $\phi_v=58\%$ : (a) flexural strength and (b) compressive strength.

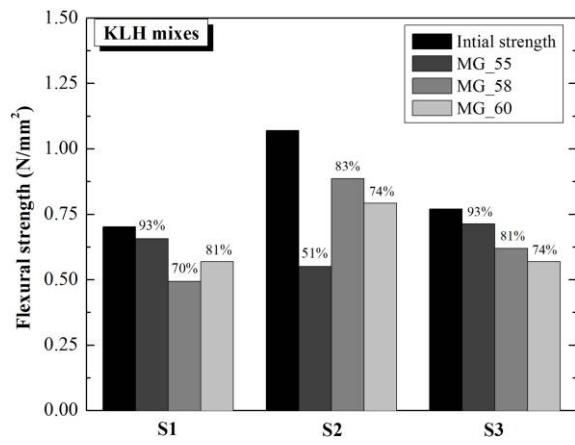


Fig. 19 – Repair efficiency of the selected mud grouts for the three soil types.

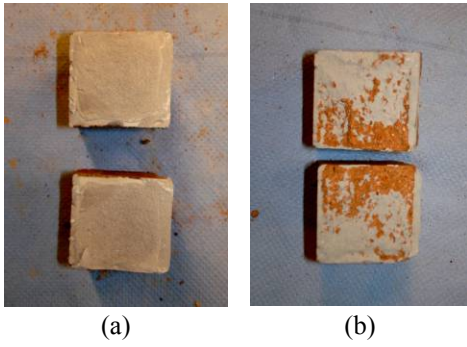


Fig. 20 – Failure mode of the repaired earthen beams: (a) failure of the grout and (b) failure of the grout-earthen beam interface.